

Lensless Fourier-transform ghost imaging with classical incoherent light

Minghui Zhang, Qing Wei, Xia Shen, Yongfeng Liu, Honglin Liu, Jing Cheng, and Shensheng Han*
*Key Laboratory for Quantum Optics and Center for Cold Atom Physics, Shanghai Institute of Optics and Fine Mechanics,
 Chinese Academy of Sciences, Shanghai 201800, China*

(Received 12 September 2006; published 20 February 2007)

The Fourier-transform ghost imaging of both amplitude-only and pure-phase objects was experimentally observed with classical incoherent light at Fresnel distance by a lensless scheme. The experimental results are in good agreement with the standard Fourier transform of the corresponding objects. This scheme provides a route toward aberration-free diffraction-limited three-dimensional images with classically incoherent thermal light (or neutrons), which have no resolution and depth-of-field limitations of lens-based tomographic systems.

DOI: [10.1103/PhysRevA.75.021803](https://doi.org/10.1103/PhysRevA.75.021803)

PACS number(s): 42.30.Va, 42.30.Rx, 42.50.Ar

X-ray crystallography has had a tremendous impact in materials sciences, structural biology, and other areas, but is applicable only to structures with periodic repeats. Samples which are difficult to crystallize are, hence, not currently accessible by x-ray crystallography. The rapid development of nanoscience and biology has produced an urgent need for techniques capable of revealing the internal structure, in three dimensions, of inorganic nanostructures and large molecules which cannot be easily crystallized (such as the membrane proteins). Scanning probe methods are limited to the studies of surface structures; electron microscopy provides atomic resolution images of crystalline materials in thicknesses up to about 50 nm or tomography of macromolecular assemblies and inorganics at lower resolution. Coherent x-ray diffraction imaging (CXDI), the combination of the coherent x-ray diffraction with the oversampling phasing method [1–7], has the potential to provide three-dimensional (3D) imaging with nanometer resolution for inherently non-periodic objects whose diffraction patterns are continuous functions [2]. The method has become available by the development of high-brilliance third-generation sources of synchrotron radiation and the development of iterative algorithms with feedback in the early 1980s [8], and the inversion of a diffraction pattern offers aberration-free diffraction-limited 3D images without limitations on the resolution and depth-of-field of lens-based tomographic systems.

The CXDI method is strongly correlated to the coherence of the incident x rays. But the perfect coherent light source of hard x rays (hard x-ray laser) is still a dream to the science community because of the required ultrahigh pumping power [9]. Fourth-generation sources (x-ray free electron laser) are now believed to be necessary for CXDI to image thick 3D objects with atomic resolution. Unlike x rays which are scattered by electrons and are nearly blind to atoms with a few electrons, neutrons scatter mainly from nuclei, which gives directly the positions of nuclei and all kinds of atoms are visible with neutron diffraction [10–12]. But an intensive coherent source for neutrons is impossible in principle because they are fermions. So a lensless diffraction scheme

which can give out Fourier diffraction patterns with incoherent thermal illumination will be very important for x-ray and neutron diffraction tomography.

On the other hand, when an object is illuminated by coherent light, it is well known that only when the Fraunhofer criterion is satisfied can the Fourier transform of the complex amplitude emerging from the object be applied to the observation plane. When the illuminating wavelength is 1 nm, for a 1-mm-wide square aperture, the Fraunhofer diffraction integral is valid only at the observing distance $z \gg 3$ km. In the visible light range, an aberration-free positive lens is frequently used to move and compress the Fraunhofer region into a space near the focal plane of the lens [13]. If aberration-free optical components, such as in x-ray wavelengths, are not available, to perform an exact optical Fourier transfer of an object based on free space propagation is difficult or practically impossible for large samples because of the unpractical, long Fraunhofer distance, even if the coherent x ray is obtainable. A method to retrieve Fourier diffraction patterns at the Fresnel distance based on free space propagation will also be very valuable for practical applications of x-ray diffraction imaging.

Conventionally, both amplitude and intensity interferometric methods have been applied in obtaining interference-diffraction patterns of a nonperiodic object where coherent, at least partially coherent, illumination is usually considered to be necessary [14]. In 1994, Belinsky and Klyshko [15] found that “ghost” diffraction imaging can be performed with entangled incoherent light by exploiting the spatial correlation between two entangled photons created by parametric down-conversion (PDC). The role of entanglement and the quantum nature in coincidence ghost imaging has led to some interesting debates [16–28]. At present, it is generally accepted that both classical thermally emitted light and quantum-entangled beams can be used for ghost imaging and ghost diffraction. A lensless Fourier-transform ghost imaging scheme was proposed and its potential applications to x-ray diffractive imaging has already been discussed [24]. Other lensless intensity correlation imaging schemes with classical thermal light were also proposed. But no diffraction pattern [21] or diffraction pattern of the phase object [29] can be retrieved from their correlation measurements, which makes the schemes unsuitable for x-ray diffractive imaging.

Ghost imaging and ghost diffraction of amplitude-only objects with classical thermal light have been examined ex-

*Corresponding author. Electronic address: sshan@mail.shnc.ac.cn

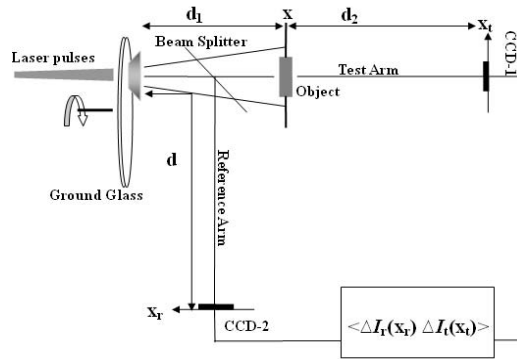


FIG. 1. The experimental setup for the lensless Fourier-transform ghost imaging.

perimentally [19,21,22,26–32]. Experimental evidence of lensless Fresnel-transformed ghost imaging of a pure-phase object with entangled photons and lens-based ghost diffractive imaging of a pure-phase object with classical thermal light have also been reported [28,33].

In this Rapid Communication, we report on the results of an experimental demonstration of lensless Fourier-transform ghost imaging of amplitude-only and pure-phase objects with classical incoherent light. We show that merely based on free space propagation, the Fourier-transform diffraction patterns of both amplitude-only and pure-phase objects illuminated by incoherent light can be extracted from the intensity correlation measured at the Fresnel observation distance.

The theoretical part of the lensless Fourier-transform ghost imaging scheme has been published previously [24], and the experimental setup is shown in Fig. 1. Based on the advanced wave concept [15,17], the light can be considered to start from the point detector at the object arm, to propagate backward in time until the source of thermal light, and then to propagate forward in time toward the space-resolve detector in the reference arm. Two key points to understand the scheme are that (i) radiation from a point like source is coherent in space (this ensures the retrieval of diffraction patterns for both amplitude and phase objects) and (ii) unlike entangled sources, thermal light sources behave as a phase-conjugate mirror [22]; this “phase-conjugate mirror” will compress the propagation of light after thermal light source and make the retrieving of Fourier diffraction patterns at the Fresnel distance possible. The pseudothermal source in the experiment is obtained by illuminating a pulsed Nd:YAG laser beam with a wavelength of $0.532 \mu\text{m}$ into a slowly rotating ground glass. A nonpolarizing beam splitter splits the radiation into two distinct optical paths. In the test arm, an amplitude-only or pure-phase object is placed at a distance $d_1=60 \text{ mm}$ from the ground glass and a charge-coupled-device (CCD) camera is placed at a distance $d_2=75 \text{ mm}$ from the object. In the reference arm, nothing but another CCD camera is placed at a distance $d=135 \text{ mm}$ from the ground glass. Here $d=d_1+d_2$ as was required by [24].

The laser pulse width was about 5 ns, and the exposure time window for the two CCD cameras was set to be 1 ms in order to ensure the detection of the signals with 5 ns pulsed width. The interval between laser pulses is, in the experiment, longer than the correlation time of the speckle pattern

determined by the rotation speed of the ground glass and the diameter of the laser spot illuminated on the ground glass, so that each data acquisition corresponds to an independent speckle pattern. The uncertainty of the time synchronization of the whole system is less than $5 \mu\text{s}$.

The transverse coherence length of the pseudothermal radiation at the object plane was found to be $10.7 \mu\text{m}$ by measuring the autocorrelation function of the speckle pattern, which is in good agreement with the value estimated from $\Delta x_{obj} \propto \lambda d_1/d_0 \approx 10.6 \mu\text{m}$; here, d_0 is the diameter of laser spot on the ground glass [34]. The Δx_{obj} is much shorter than the feature size of the objects used in the experiment, implying that the objects were illuminated by a classic incoherent light.

A Young’s double slit was used in the experiment as amplitude-only objects. The two slits are separated by $302 \mu\text{m}$ and have a width of $105 \mu\text{m}$. The pure-phase object was made by etching two grooves with width of $150 \mu\text{m}$ and separated by $300 \mu\text{m}$ on a quartz glass. Since the wavelength of the pseudothermal light is $0.532 \mu\text{m}$, the depth of two grooves was designed to be $\lambda/2(n-1)=0.532/2(1.57-1)=0.46 \mu\text{m}$ to form a phase difference of $\Delta\phi=\pi$ to the unetched area.

No diffraction patterns, as shown in Figs. 2(a) and 3(a), can be observed when the objects were illuminated by pseudothermal light. Figures 2(b) and 3(b) are 2D diffraction patterns (upper left) and their cross-section curves (lower right) of amplitude-only and pure-phase objects which are directly illuminated by the coherent laser pulses. Because the distance from the object plane to the CCD camera in the test arm is so short, only Fresnel diffraction patterns can be observed.

According to [24], when $d=d_1+d_2$, the Fourier-transform modulus of an object can be obtained by correlating the acquired intensity fluctuation distribution of the reference arm with the intensity fluctuation of a fixed point in the test arm:

$$\langle \Delta I_r(x_r) \Delta I_t(0) \rangle = \frac{I_0^2}{\lambda^4 d_2^4} \left| T \left(\frac{-2\pi x_r}{\lambda d_2} \right) \right|^2. \quad (1)$$

Here $T \left(\frac{-2\pi x_r}{\lambda d_2} \right)$ is the Fourier transformation of the observed object.

Shown in Figs. 2(c) and 3(c) are the Fourier-transform diffraction patterns of both amplitude-only and pure-phase objects after averaging the cross correlation over 10 000 samples.

The quality of the retrieved Fraunhofer diffraction patterns is obviously comparable with that of Fresnel diffraction patterns obtained by directly illuminating the objects with a laser beam, and the cross-section curves of these diffraction patterns are in good agreement with theoretical results of the corresponding objects’ Fourier-transform. Notice that the differences between Fresnel and Fraunhofer diffraction patterns are obvious, especially for the pure-phase object. The Fourier transform diffraction patterns obtained with a standard coherent single-lens $2-f$ system (Chapter 5 of Ref. [13]) ($f=75 \text{ mm}$) are also shown in Figs. 2(d) and 3(d), respectively, for comparison. In all the experiments, the spatial average has been involved to improve the convergence rate.

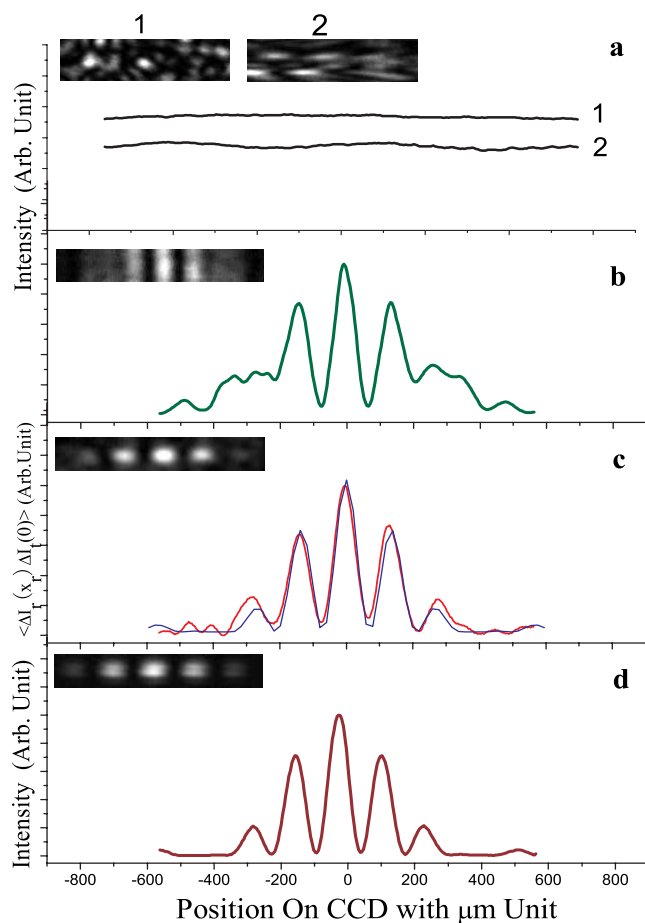


FIG. 2. (Color) Reconstruction of the diffraction pattern of an amplitude-only object via correlation measurements (a). Instantaneous intensity distribution (top) and the cross sections of the averaged intensity distribution (bottom) of (1) reference arm and (2) test arm when the amplitude-only object was illuminated by pseudothermal light. (b) Fresnel diffraction pattern (upper left) and its cross-section curve recorded in the test arm when the Young's double slit was illuminated by a laser. (c) Fourier-transform diffraction pattern (upper left) and its cross-section curve (red line) obtained by the cross correlation of the intensity fluctuations when the object was illuminated by pseudothermal light. Numerical results from Fraunhofer diffraction integral (blue line) are also shown. (d) Standard Fourier-transform pattern (upper left) and its cross-section curve obtained by a single-lens $2-f$ system ($f=75$ mm) illuminated by a laser.

In addition, based on Fienup's iterative algorithm [1], both amplitude-only and pure-phase objects can be retrieved from the experimental Fourier-transform diffraction patterns as show in Fig. 4.

Thus, our experimental results clearly show that, though recorded in the Fresnel region and without introducing any converging optical elements, high-resolution Fourier-transform diffraction patterns of amplitude- and phase-modulated objects both can be perfectly reconstructed from the cross correlation of the test-reference intensity fluctuations when the object is illuminated by a classic incoherent thermal light and the diffraction patterns are qualified enough to retrieve images in spatial domain.

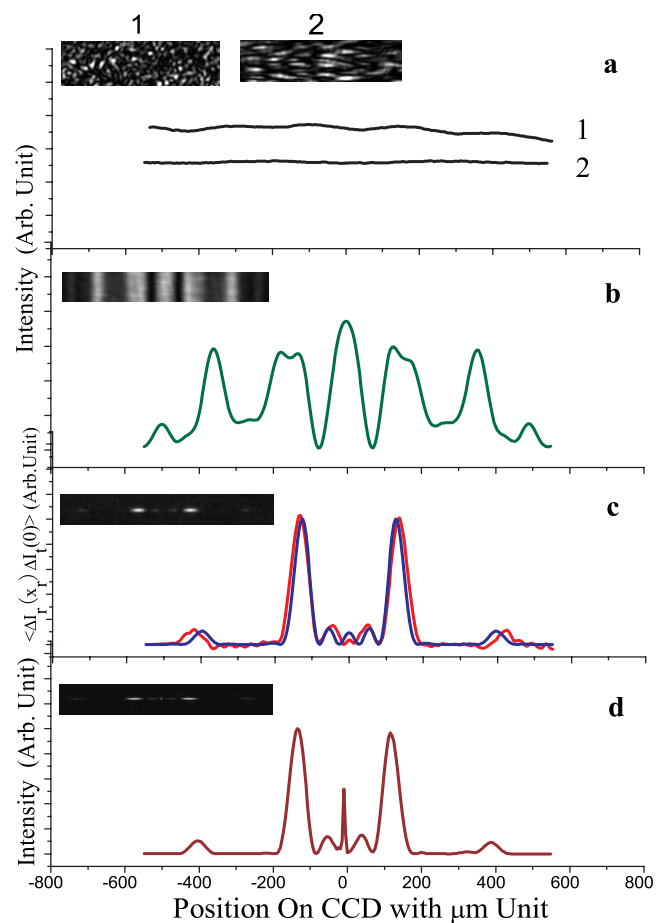


FIG. 3. (Color) Reconstruction of the diffraction pattern of a pure-phase object via correlation measurements (a). Instantaneous intensity distribution (top) and the cross sections of the averaged intensity distribution (bottom) of (1) reference arm and (2) test arm when the pure-phase object was illuminated by pseudothermal light. (b) Fresnel diffraction patterns (upper left) and its cross-section curve recorded in the test arm when the object was illuminated by a laser. (c) Fourier-transform diffraction pattern (upper left) and its cross-section curve (red line) obtained by the cross correlation of the intensity fluctuations when the pure-phase object was illuminated by pseudothermal light. Numerical results from Fraunhofer diffraction integral (blue line) are also presented. (d) Standard Fourier-transform patterns (upper left) and its cross-section curve obtained by a single-lens $2-f$ system ($f=75$ mm) when illuminated by a laser.

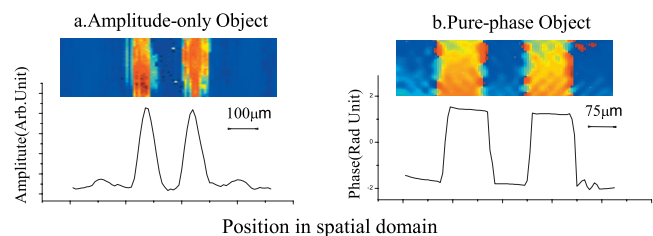


FIG. 4. (Color) Images in spatial domain retrieved from diffraction patterns obtained by the lensless Fourier-transform ghost imaging scheme. Pseudocolor patterns and their profiles are in accordance with their spatial features for (a) amplitude-only object and (b) pure-phase object.

Lensless Fourier-transform ghost imaging with classical thermal light for both amplitude, and pure-phase-modulated objects recorded at the Fresnel distance have been experimentally demonstrated. Combined with rapidly developed inversion algorithms of diffraction patterns, the scheme provides a route toward aberration-free diffraction-limited 3D images with classically incoherent thermal light, which have no resolution and depth-of-field limitations of lens-based tomographic systems. The coherence time of a monochromatic light $\tau_c = \lambda^2 / (\Delta\lambda c)$, where c is the light speed in vacuum. For $\lambda = 1$ nm, $\lambda / \Delta\lambda = 3000$, the coherent time of the x-ray pulse would be 10 fs. A femtosecond tabletop terawatt laser facility that can be used to generate ultra-bright femtosecond

x-ray pulses is routinely available [35,36]. So a tabletop x-ray diffractive imaging system with a similar experimental setup is possible. We believe that the scheme can also be extended to fermions where intensive coherence sources are impossible in principle.

S.H. thanks Professor Da-ming Zhu for stimulated discussions when preparing the manuscript and Professor Yang-chao Tian for preparing the phase objects. This research is partly supported by the National Natural Science Foundation of China, Project No. 60477007, the Shanghai Optical-Tech Special Project, Project No. 034119815, and Shanghai Fundamental Research Project (06JC14069).

-
- [1] V. Elser, *J. Opt. Soc. Am. A* **20**, 40 (2003).
 [2] S. Marchesini, H. N. Chapman, S. P. Hau-Riege, R. A. London, and A. Szoke, *Opt. Express* **11**, 2344 (2003); J. Cheng and S. Han, *J. Opt. Soc. Am. A* **18**, 1460 (2001).
 [3] G. J. Williams, M. A. Pfeifer, I. A. Vartanyants, and I. K. Robinson, *Phys. Rev. Lett.* **90**, 175501 (2003).
 [4] J. Miao, T. Ishikawa, B. Johnson, E. H. Anderson, B. Lai, and K. O. Hodgson, *Phys. Rev. Lett.* **89**, 088303 (2002).
 [5] I. K. Robinson, I. A. Vartanyants, G. J. Williams, M. A. Pfeifer, and J. A. Pitney, *Phys. Rev. Lett.* **87**, 195505 (2001).
 [6] J. Miao, P. Charalambous, J. Kirz, and D. Sayre, *Nature (London)* **400**, 344 (1999).
 [7] J. Miao, D. Sayre, and H. N. Chapman, *J. Opt. Soc. Am. A* **15**, 1662 (1998).
 [8] J. R. Fienup, *Appl. Opt.* **21**, 2758 (1982).
 [9] R. C. Elton, *X-Ray Lasers* (Academic, San Diego, 1990).
 [10] G. E. Bacon, *Neutron Diffraction* (Oxford University Press, London, 1975).
 [11] C. G. Shull, *Rev. Mod. Phys.* **67**, 753 (1995).
 [12] B. Sur *et al.*, *Nature (London)* **414**, 525 (2001).
 [13] J. W. Goodman, *Introduction to Fourier Optics* (McGraw-Hill, San Francisco, 1968).
 [14] J. W. Goodman, *Statistical Optics* (Wiley, New York, 1985).
 [15] A. V. Belinsky and D. N. Klyshko, *J. Exp. Theor. Phys.* **78**, 259 (1994).
 [16] A. Gatti, E. Brambilla, and L. A. Lugiato, *Phys. Rev. Lett.* **90**, 133603 (2003).
 [17] T. B. Pittman, Y. H. Shih, D. V. Strekalov, and A. V. Sergienko, *Phys. Rev. A* **52**, R3429 (1995).
 [18] A. F. Abouraddy, B. E. A. Saleh, A. V. Sergienko, and M. C. Teich, *Phys. Rev. Lett.* **87**, 123602 (2001).
 [19] R. S. Bennink, S. J. Bentley, and R. W. Boyd, *Phys. Rev. Lett.* **89**, 113601 (2002).
 [20] R. S. Bennink, S. J. Bentley, R. W. Boyd, and J. C. Howell, *Phys. Rev. Lett.* **92**, 033601 (2004).
 [21] G. Scarcelli, V. Berardi, and Y. Shih, *Phys. Rev. Lett.* **96**, 063602 (2006).
 [22] G. Scarcelli, V. Berardi, and Y. Shih, *Appl. Phys. Lett.* **88**, 061106 (2006).
 [23] M. D'Angelo, Y.-H. Kim, S. P. Kulik, and Y. Shih, *Phys. Rev. Lett.* **92**, 233601 (2004).
 [24] J. Cheng and S. Han, *Phys. Rev. Lett.* **92**, 093903 (2004).
 [25] A. Gatti, E. Brambilla, M. Bache, and L. A. Lugiato, *Phys. Rev. Lett.* **93**, 093602 (2004).
 [26] G. Scarcelli, A. Valencia, and Y. Shih, *Europhys. Lett.* **68**, 618 (2004).
 [27] A. Gatti, M. Bache, D. Magatti, E. Brambilla, F. Ferri, and L. A. Lugiato, *J. Mod. Opt.* **53**, 739 (2006).
 [28] M. Bache, D. Magatti, F. Ferri, A. Gatti, E. Brambilla, and L. A. Lugiato, *Phys. Rev. A* **73**, 053802 (2006).
 [29] K. Wang and D.-Z. Cao, *Phys. Rev. A* **70**, 041801(R) (2004); J. Xiong, D.-Z. Cao, F. Huang, H.-G. Li, X.-J. Sun, and K. Wang, *Phys. Rev. Lett.* **94**, 173601 (2005).
 [30] F. Ferri, D. Magatti, A. Gatti, M. Bache, E. Brambilla, and L. A. Lugiato, *Phys. Rev. Lett.* **94**, 183602 (2005).
 [31] A. Valencia, G. Scarcelli, M. D'Angelo, and Y. Shih, *Phys. Rev. Lett.* **94**, 063601 (2005).
 [32] Y.-H. Zhai, X.-H. Chen, D. Zhang, and L.-A. Wu, *Phys. Rev. A* **72**, 043805 (2005); D. Zhang, Y.-H. Zhai, L.-A. Wu, and X.-H. Chen, *Opt. Lett.* **30**, 2354 (2005).
 [33] A. F. Abouraddy, P. R. Stone, A. V. Sergienko, B. E. A. Saleh, and M. C. Teich, *Phys. Rev. Lett.* **93**, 213903 (2004).
 [34] J. W. Goodman, in *Statistical Properties of Laser Speckle Patterns*, edited by J. C. Dainty, Laser Speckle and Related Phenomena Vol. 9 (Springer-Verlag, Heidelberg, 1975).
 [35] M. D. Perry and G. Mourou, *Science* **264**, 917 (1994).
 [36] G. A. Mourou, T. Tajima, and S. V. Bulanov, *Rev. Mod. Phys.* **78**, 309 (2006).